Published in final edited form as:
J Phys Chem C Nanomater Interfaces. 2010 March 5; 114(14): 6396–6400. doi:10.1021/jp100354z.

Dissolving Ag from Au-Ag Alloy Nanoboxes with H_2O_2: A Method for Both Tailoring the Optical Properties and Measuring the H_2O_2 Concentration

Qiang Zhang[†,‡], **Claire M. Cobley**[†], **Jie Zeng**[†], **Long-Ping Wen**[‡], **Jingyi Chen**[†,*], and **Younan Xia**[†,*]

[†]Department of Biomedical Engineering, Washington University, St. Louis, Missouri 63130

[‡]Hefei National Laboratory for Physical Sciences at the Microscale, University of Science and Technology of China, Hefei, Anhui 230027, P. R. China

Abstract

This article describes a method for generating Au-based nanocages with controlled wall thickness, porosity, and optical properties by dissolving Ag from Au-Ag alloy nanoboxes with H_2O_2. It involves two steps: *i*) formation of Au-Ag alloy nanoboxes with some pure Ag left behind by titrating Ag nanocubes with aqueous $HAuCl_4$; and *ii*) removal of Ag atoms from both the pure Ag remaining in the nanoboxes and the alloy walls via H_2O_2 etching. The optical properties of the resultant Au-Ag nanocages can be easily tailored by controlling the amount of H_2O_2 added into the reaction system. Due to the changes to the optical spectra, the Au-Ag alloy nanoboxes can also be employed to detect H_2O_2 with a more or less linear readout in the range of concentration from 5×10^{-2} M down to 5×10^{-7} M.

Keywords

Au-based nanoboxes; nanocages; dealloying; H_2O_2 detection

Introduction

Metallic hollow nanostructures often exhibit exceptional optical, electronic, and catalytic properties as compared to their solid counterparts due to the increased surface area, reduced density, and broadly tunable localized surface plasmon resonance (LSPR).[1] They have been actively explored for a range of applications, such as sensing, optical imaging, photothermal treatment, drug delivery, as well as catalysis.2¯6 Galvanic replacement, driven by the electrical potential difference between two metals, provides a facile method for generating metallic hollow nanostructures. Several bimetallic and tri-metallic hollow nanostructures comprised of Ag and Au, Pd, or Pt have been produced through the galvanic replacement between Ag nanostructures and salt precursors of less reactive metals such as Au, Pd, and Pt.[7,8] For example, Ag nanocubes can be titrated with an aqueous $HAuCl_4$ solution to generate Au-Ag alloy nanoboxes (structures with hollow interiors) and nanocages (structures with both hollow interiors and porous walls) with a broad range of controllable compositions. During the structural evolution from nanocubes to nanoboxes and nanocages, the LSPR peaks shift from the visible to the near-infrared (NIR) region due to the change in wall thickness relative to the overall dimension of the nanostructures.[9] In this process, the dissolution of Ag and deposition

*Corresponding authors: xia@biomed.wustl.edu; chenj@seas.wustl.edu.

of Au occur simultaneously on the same nanocube during the reaction. This coupling makes it very difficult to tune and control the wall thickness and porosity of the resultant hollow nanostructures, especially during the dealloying stage. Recently, a two-step procedure was demonstrated to solve this problem by dealloying Ag from the pre-formed Au-Ag nanoboxes (pre-formed via the galvanic replacement reaction) with an etchant such as $Fe(NO_3)_3$, NH_4OH, or thiols.[10] Unlike $HAuCl_4$, these wet etchants offer a tighter control over the wall thickness and porosity due to the elimination of Au deposition. In principle, any chemical with an electrochemical potential higher than that of Ag^+/Ag can serve as an oxidative etchant in the second step.

Hydrogen peroxide (H_2O_2) is a powerful oxidizing agent. The standard redox potential of H_2O_2 is dependent on the pH value of the solution:[11]

$$H_2O_2+2H^++2e \rightarrow 2H_2O \quad E^0=1.763\ V$$

$$H_2O_2+2e \rightarrow 2OH^- \quad E^0=0.867\ V$$

Under both conditions, the electrochemical potentials are higher than that of Ag^+/Ag (E^0 = 0.7996 V).[12] Therefore, H_2O_2 can serve as an effective etchant for elemental Ag in tailoring the optical properties of the Au-Ag alloy nanoboxes and nanocages. In addition, during the removal of Ag, the changes to optical spectra provide a simple assay for H_2O_2 detection based on a colorimetric approach. Hydrogen peroxide is involved in many biological processes and enzymatic reactions related to intracellular oxidative stress and ageing.[13–14] For example, the intracellular concentration of H_2O_2 has a profound impact on cellular physiological processes including proliferation, growth arrest, and apoptosis.[15–17] It also plays an important role in food processing as an antimicrobial agent[18] and in atmospheric science as an oxidant related to the formation of acid rain.[19] Therefore, determination of H_2O_2 concentration is essential to monitoring and understanding these biological and environmental processes.

In this study, we systematically investigated the etching of Au-Ag alloy nanoboxes, with H_2O_2 serving as an oxidant. The wall thickness of the resultant Au-based nanocages could be readily controlled by adding different amounts of H_2O_2 to the suspension of Au-Ag alloy nanoboxes that were, in turn, obtained by carrying out the galvanic replacement to different extents. The LSPR peaks of the Au-based nanocages could be conveniently tuned across the entire visible region into the near-infrared from 500 nm to 1000 nm. Based on this etching mechanism, we also demonstrated the use of the Au-Ag alloy nanoboxes as a new platform for the quantitative analysis of H_2O_2 using a spectroscopic method.

Experimental Section

Titration of Au-Ag Alloy Nanoboxes with H_2O_2

The Au-Ag alloy nanoboxes were synthesized using the galvanic replacement reaction between Ag nanocubes and $HAuCl_4$ as described previously.[10] Briefly, 15 mL of 1 mg/mL poly(vinyl pyrrolidone) (PVP, M.W. ≈ 55,000) aqueous solution was added to a 100-mL round-bottom flask and heated in an oil bath at 100 °C under stirring for 10 min. Subsequently, 100 μl of the as-synthesized Ag nanocubes of 45 nm in mean edge length (0.17 nM or 1.0×10^{14} nanocube/mL) was added to the flask. Two minutes later, 0.5 mM $HAuCl_4$ aqueous solution was introduced into the flask using a syringe pump at a rate of 45 mL/h. The titration was stopped after the extinction peak of the solution had reached 460 nm. A similar procedure was also

used to prepare Au-Ag nanoboxes with LSPR peaks being tuned to 520, 545, 675, and 745 nm, respectively.

For the reaction with H_2O_2, the as-prepared suspension of Au-Ag nanoboxes was added to a 20-mL glass vial under magnetic stirring at room temperature, followed by the addition of an excess amount of H_2O_2 solution. The reaction was allowed to proceed at room temperature for 10 min. To study the structural evolution during the reaction, the Au-Ag nanoboxes with an LSPR peak at 520 nm were titrated with different amounts of H_2O_2 solution and aliquots were taken from the solution at different time points. The products were washed using a procedure reported in a previous publication.[20]

Detection of H_2O_2 with the Au-Ag Nanoboxes

The Au-Ag nanoboxes with an LSPR peak at 545 nm were used to demonstrate H_2O_2 detection. In a typical assay, a series of H_2O_2 solutions were prepared with concentrations in the range of 1×10^{-6} to 1×10^{-1} mol/L (M). Then, 0.5 mL of the H_2O_2 solutions having various concentrations were separately added to 2-mL plastic cuvettes, followed by the introduction of 0.5 mL of the Au-Ag nanoboxes, resulting in final H_2O_2 concentrations of 5×10^{-7} M to 5×10^{-2} M. The solution in each cuvette was mixed on a shaker at room temperature for 30 min before a spectrum was taken using a UV-vis-NIR spectrometer.

Instrumentation

The sample for scanning electron microscopy (SEM) was prepared by dropping a few microliters of the particle suspension on a small piece of silicon substrate, followed by drying under ambient conditions. The SEM images and the energy-dispersive X-ray (EDX) spectra were captured using a field-emission microscope (FEI, Nova NanoSEM 230) operated at accelerating voltages of 10–20 kV. The sample for transmission electron microscopy (TEM) was prepared by replacing the silicon substrate with a carbon-coated copper grid. The TEM images were captured using a FEI G2 Spirit Twin electron microscope operated at 120 kV. The high-resolution TEM images were recorded using a JEOL 2100F electron microscope operated at 200 kV. The UV-vis-NIR spectra were taken using a Cary 50 spectrophotometer (Varian, Palo Alto, CA) or a Lambda 950 spectrophotometer (Perkin Elmer, Waltham, MA).

Results and Discussion

The essence of this study is the formation of Au-based nanocages by dissolving Ag from the Au-Ag alloy nanoboxes with an excess amount of H_2O_2. Prior to the addition of H_2O_2, the Au-Ag nanoboxes were prepared using the galvanic replacement reaction between Ag nanocubes and $HAuCl_4$. Figure 1, A–D, shows TEM images of the Au-Ag alloy nanoboxes with increased void sizes that were synthesized by titrating suspensions of Ag nanocubes (of the same volume) with different amounts of $HAuCl_4$. During the replacement reaction, three Ag atoms were removed while one Au atom was formed and deposited on the surface of the Ag nanocube. As a result, a pit was initially formed on the surface of the nanocube. It is known that Ag atoms can diffuse into the lattice of Au to form a thin layer of Au-Ag alloy at the surface.[21] At an intermediate stage, the pit could evolve into a void inside the nanocube, resulting in the formation of a Au-Ag nanobox with some pure Ag remaining in the Au-Ag alloy nanobox.

In the first set of experiments, an excess amount of H_2O_2 was introduced as an oxidant to etch away elemental Ag from both the remaining pure Ag and the Au-Ag alloy walls (Figure 1, E–H). The dissolution of Ag is based on the following reaction at pH = 6:

$$2Ag+H_2O_2 \rightarrow 2Ag^+ + 2OH^- \quad \Delta E^0 = 0.067\ V$$

The remaining pure Ag inside each Au-Ag alloy nanobox and the Ag in the Au-Ag alloy walls could both be dissolved without additional deposition of Au atoms. As a result, the wall thickness and porosity of the Au nanocages can be more easily controlled. Depending on the amount of $HAuCl_4$ added in the first step, the wall thickness of the resultant nanocages was tuned to 2.5, 3.5, 4.5 and 6.5 nm, respectively (Figure 1, E–H). Note that the nanocages in Figure 1, E and F, were slightly distorted because their walls were too thin to survive the strong capillary force induced by solvent evaporation during TEM sample preparation. These nanostructures were also more porous than those shown in Figure 1, G and H, because of their further reduced wall thickness. EDX analysis indicates that the percentages of Au atoms in the nanocages were 23, 44, 46 and 66%, respectively, for the samples shown in Figure 1, E–H. This result suggests that H_2O_2 could not completely remove Ag atoms from the Au-Ag alloy walls, which is different from our previous study that involved the use of $Fe(NO_3)_3$ as an etchant.[10] This incompleteness might be due to the oxidation of surface Ag atoms or the formation of a by-product such as AgOH or Ag_2O that might hinder the further removal of Ag from the alloy walls. Additionally, it might also be related to the change in redox potential as the composition of the Au-Ag alloy nanoboxes was altered.

Figure 2 shows a TEM image and a typical high-resolution TEM image taken from the corner of a nanocage. The well-resolved, continuous lattice fringe (2.0 Å in spacing) parallel to the edges of the nanocage indicates that the nanocage was a single-crystal made of Ag-Au alloy. Comparing to the previous work based on $Fe(NO_3)_3$,[10] there are three major advantages for using H_2O_2 as an etchant: *i*) the wall thickness of the nanocage can be conveniently tuned down to 2.5 nm, with an accuracy of ±0.5 nm; *ii*) the Au nanocage retained its well-defined, box-type shape in stead of being transformed into a frame-like structure; and *iii*) the elimination of a possible source of contamination from the Fe ions that might compromise the performance of Au nanocages in various applications.

We then studied the optical properties of the as-prepared Au-Ag alloy nanostructures by UV-vis-NIR spectroscopy. Figure 3 shows the UV-vis-NIR spectra of Au-Ag nanoboxes before and after treatment with an excess amount of H_2O_2, corresponding to the structures shown in Figure 1. The LSPR peaks of the Au-Ag alloy nanoboxes in Figure 1, A–D, were located at 460, 520, 675, and 745 nm, respectively. After the treatment with excess H_2O_2, the peaks were red-shifted to 1210, 925, 790, and 758 nm, respectively, for the samples in Figure 1, E–H. The corresponding intensities of the peaks were reduced from 1.0 to 0.13, 0.18, 0.58 and 0.74, respectively. This trend is in agreement with our previously published calculation based on discrete-dipole-approximation (DDA): that is, the LSPR peak tends to red-shift as the wall thickness is reduced, and the intensity of the peak drops as the walls became thinner and more porous.[22] Additionally, the full width at half maximum (FWHM) of the LSPR peak became broader as the wall thickness decreased. The increased broadening can be attributed to a combination of surface scattering of electrons, as well as increased radiation damping for the nanoboxes.23 This effect is more pronounced when the wall thickness is below 5 nm.

To fully understand the etching process, we also studied the structural evolution from the nanobox to nanocage during the titration with H_2O_2. Figure 4 shows TEM images of Au-Ag alloy nanoboxes with an LSPR peak at 520 nm after treatment with different amounts of H_2O_2: 0, 10, 20, 30, 40, and 50 μL of 10 mM H_2O_2, respectively. As more H_2O_2 was titrated into the reaction, the void size in the interior of each nanobox gradually increased due to the dissolution of the remaining Ag (Figure 4, B and C). After the pure Ag had been completely removed from the inside, the H_2O_2 started to dissolve Ag atoms from the alloyed walls. As a result, the walls became porous, resulting in the formation of Au-based nanocages. For the sample shown in Figure 4F, the nanocages contained 44% Au and 56% Ag. Figure 5 shows the corresponding UV-vis-NIR spectra for the samples shown in Figure 4, clearly indicating that the LSPR peaks were shifted to 617, 691, 850, 901, and 963 nm.

The spectral changes observed for the Au-Ag alloy nanoboxes can be applied to develop a colorimetric method for the detection of H_2O_2. After the addition of H_2O_2, the absorbance spectrum of the nanoboxes displayed two major changes: *i*) drop of the LSPR peak intensity, and *ii*) red-shift of the peak position. We tested the sensitivity of detection for Au-Ag alloy nanoboxes with their LSPR peaks being tuned to 545, 660 and 750 nm, respectively. Figure 6A shows the time-dependent study with H_2O_2 treatment to determine the best reaction time for the assay. At a concentration of 0.1 M, the intensity of the peak decreased rapidly in the first 20 min and levered off in 30 min after the addition of H_2O_2. This observation suggested that the reaction between H_2O_2 and Ag were completed in 30 min. We therefore chose 30 min to be the incubation time for the assay. In a typical procedure, 0.5 mL H_2O_2 aqueous solution at a concentration ranging from 0.1 M to 10^{-6} M was added into each cuvette, followed by the addition of 0.5 mL suspension of the Au-Ag alloy nanoboxes, resulting in final H_2O_2 concentrations in the range of 5×10^{-2} M to 5×10^{-7} M. After incubation for 30 min on a shaker, a UV-vis-NIR spectrum was measured for each reaction. The intensity of the absorbance peak at 545 nm decreased gradually as a function of H_2O_2 concentration (Figure 6B). In the case of the other two samples of Au-Ag alloy nanoboxes with the LSPR peaks at 660 and 750 nm, the intensity change for the absorbance peak was very small when the concentration of H_2O_2 was low, possiblely due to the presence of a large portion of Ag in the alloy walls (Figure S1). As a result, we chose Au-Ag alloy nanoboxes with the LSPR peak at 545 nm for the detection of H_2O_2. We plotted the absorbance change (ΔAbs) as a function of p[M], where p[M] is defined as the negative decimal logarithm of the H_2O_2 concentration in an aqueous solution (Figure 6C). The ΔAbs linearly decreased with p[M] in the concentration range from 5×10^{-2} to 5×10^{-7} M, $\Delta\text{Abs} = 0.28 - 0.03 \times \text{p[M]}$, $R^2 = 0.99$. This linear dependence offers a simple method for reading out the concentration of H_2O_2. The detection of H_2O_2 is based on an electrochemical process, in which the remaining pure Ag in the Au-Ag alloy box was oxidized by the H_2O_2, resulting in changes to the optical spectrum. In other words, the intensity of the absorbance peak decreases at 545 nm due to the dissolution of pure Ag, accompanied by the rise of absorbance peak at longer wavelengths because the structure became more empty. This method may provide some advantages over the currently existing methods,[24–26] for example, the possibility for a direct, quantitative measurement of H_2O_2 without adding special reagents, easiness of operation, and relatively low cost.

Conclusion

We have demonstrated a facile method for preparing Au-based alloy nanocages with well-controlled wall thickness and porosity by gradually dissolving the Ag from Au-Ag alloy nanoboxes with H_2O_2. For the nanocages with an inner edge length of 45 nm, the wall thickness could be conveniently tuned from 6.5 nm to 2.5 nm with the corresponding LSPR peaks being red-shifted from 758 to 1210 nm. Addition of an excess amount of H_2O_2 resulted in the formation of porous nanocages with relatively sharp corners, rather than the formation of nanoframe as in the case of etching with $Fe(NO_3)_3$. By using this method, we can easily produce the well-defined nanocages with ultrathin walls which could be a better candidate for catalysis.[27] Additionally, when a specific amount of Au-Ag alloy nanoboxes was used, the intensity of the LSPR peak decreased linearly as the concentration of H_2O_2 was increased in the range of 5×10^{-7} to 5×10^{-2} M, suggesting that the Au/Ag alloy nanoboxes can potentially serve as new platform for H_2O_2 detection.

Supplementary Material

Refer to Web version on PubMed Central for supplementary material.

Acknowledgments

This work was supported in part by a 2006 Director's Pioneer Award from the NIH (DP1 OD000798) and startup funds from Washington University in St. Louis. As a visiting student from the University of Science and Technology of China, Q.Z. was also partially supported by the China Scholarship Council. Part of the work was performed at the Nano Research Facility (NRF), a member of the National Nanotechnology Infrastructure Network (NNIN), which is supported by the NSF under award no. ECS-0335765. We thank Prof. Richard Loomis for allowing us to use the UV-vis-NIR spectrometer in his laboratory.

References

1. Skrabalak SE, Chen J, Sun Y, Lu X, Au L, Cobley CM, Xia Y. Acc. Chem. Res 2008;41:1587–1595. [PubMed: 18570442]
2. Sun Y, Xia Y. Anal. Chem 2002;74:5297–5305. [PubMed: 12403584]
3. Chen J, Saeki F, Wiley BJ, Cang H, Cobb MJ, Li Z-Y, Au L, Zhang H, Kimmey MB, Li X, Xia Y. Nano Lett 2005;5:473–477. [PubMed: 15755097]
4. Chen J, Wang D, Xi J, Au L, Siekkinen A, Warsen A, Li Z-Y, Zhang H, Xia Y, Li X. Nano Lett 2007;7:1318–1322. [PubMed: 17430005]
5. Hirsch LR, Gobin AM, Lowery AR, Tam F, Drezek RA, Halas NJ, West JL. Ann. Biomed. Eng 2006;34:15–22. [PubMed: 16528617]
6. Cobley CM, Campbell DJ, Xia Y. Adv. Mater 2008;4:748–752. [PubMed: 18568091]
7. Chen J, McLellan JM, Siekkinen A, Xiong Y, Li Z-Y, Xia Y. J. Am. Chem. Soc 2006;128:14776–14777. [PubMed: 17105266]
8. Chen J, Wiley B, McLellan J, Xiong Y, Li Z-Y, Xia Y. Nano Lett 2005;5:2058–2062. [PubMed: 16218737]
9. Sun Y, Xia Y. Nano Lett 2003;3:1569–1572.
10. Lu X, Au L, McLellan J, Li Z-Y, Marquez M, Xia Y. Nano Lett 2007;7:1764–1769. [PubMed: 17489641]
11. Tratnyek PG, Macalady DL. Handbook of Property Estimation Methods for Chemicals: Environmental and Health Sciences. 2000
12. Som T, Karmakar B. Nano Res 2009;2:607–616.
13. Fang J, Sawa T, Akaike T, Maeda H. Cancer Res 2002;62:3138–3143. [PubMed: 12036926]
14. Delaunay A, Pflieger D, Barrault M, Vinh J, Toledano MB. Cell 2002;111:471–481. [PubMed: 12437921]
15. Finkel T, Holbrook NJ. Nature 2000;408:239–247. [PubMed: 11089981]
16. Deng X, Gao F, May WS Jr. Blood 2003;102:3179–3185. [PubMed: 12855558]
17. Veal EA, Day AM, Morgan BA. Mol. Cell Rev 2007;26:1–14.
18. Welk A, Meller C, Schubert R, Schwahn C, Kramer A, Below H. BMC Microbiol 2009;9:1–8. [PubMed: 19121223]
19. Lee M, Heikes BG, O'Sullivan DW. Atmos. Environ 2000;34:3475–3494.
20. Skrabalak SE, Au L, Li X, Xia Y. Nat. Protoc 2007;2:2183–2190.
21. Sun Y, Xia Y. J. Am. Chem. Soc 2004;126:3892–3901. [PubMed: 15038743]
22. Chen J, Wiley B, Li Z-Y, Campbell D, Saeki F, Cang H, Au L, Lee J, Li X, Xia Y. Adv. Mater 2005;17:2255–2261.
23. Hu M, Petrova H, Siekkinen AR, Chen J, McLellan JM, Li Z-Y, Marquez M, Li X, Xia Y, Hartland GVJ. J. Phys. Chem. B 2006;110:19923–19928. [PubMed: 17020378]
24. Hurdis E, Romeyn H Jr. Anal. Chem 1954;26:320–325.
25. Gou S, Wang E. Anal. Chim. Acta 2007;598:181–192. [PubMed: 17719891]
26. Hanaoka S, Lin J, Yamada M. Anal. Chim. Acta 2001;426:57–64.
27. Zeng J, Zhang Q, Chen J, Xia Y. Nano Lett 2010;10:30–35. [PubMed: 19928909]

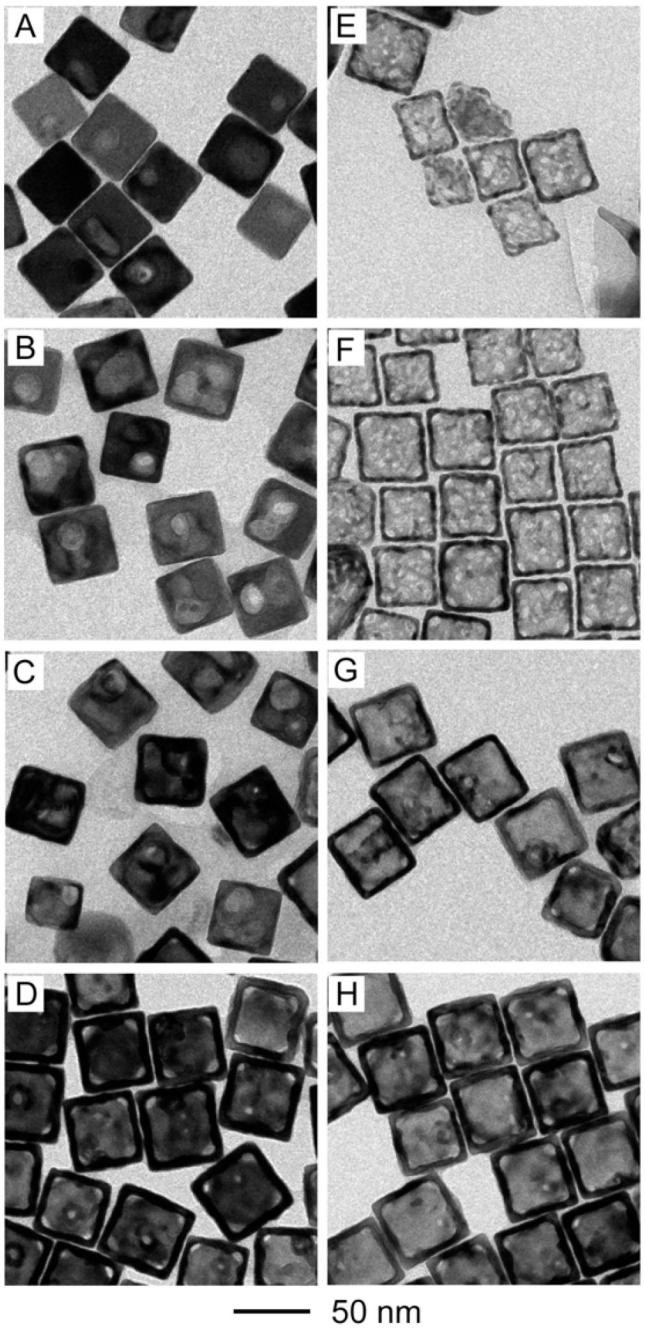

Figure 1.
TEM images of Au-Ag nanoboxes before and after etching with an excess amount of H_2O_2: (A–D) the Au-Ag nanoboxes with their LSPR peaks being tuned to 460, 520, 675 and 745 nm, respectively, prior to the addition of H_2O_2, and (E–H) the corresponding Au-based nanocages after the addition of excess H_2O_2.

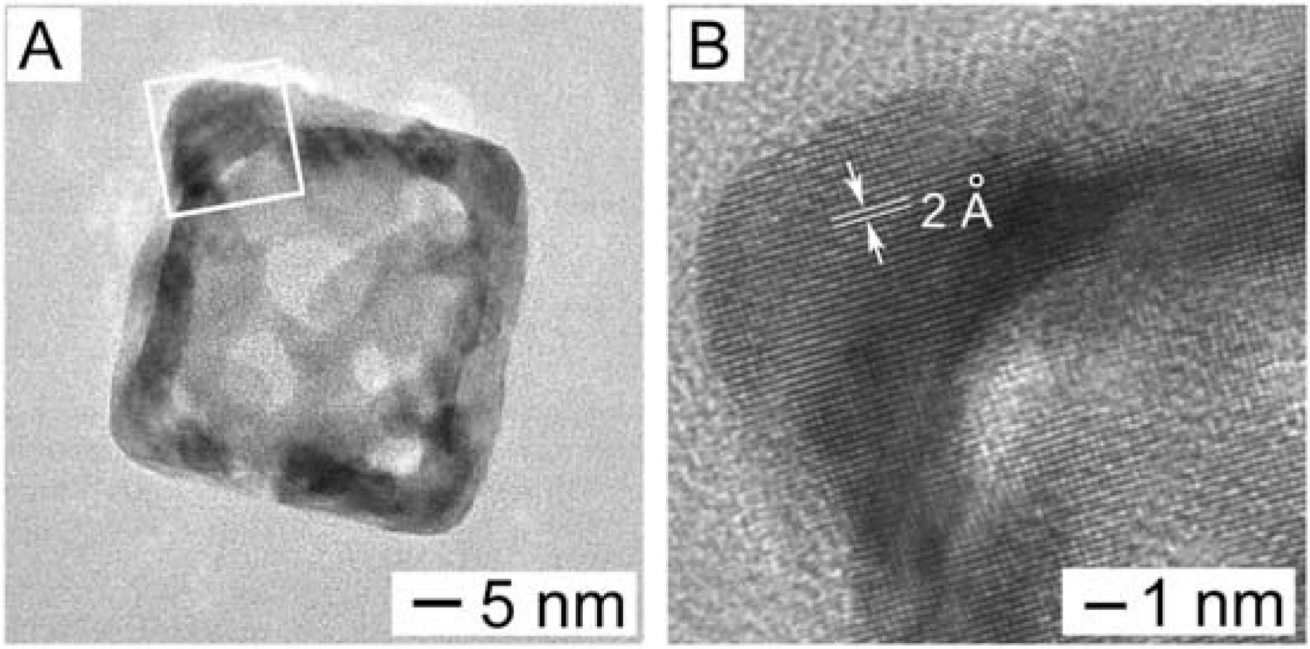

Figure 2.
(A) TEM image of a representative nanocage (from the sample shown in Figure 1F) synthesized by partially dissolving Ag from the Au-Ag nanobox with excess H_2O_2. (B) High-resolution TEM image of the area boxed in (A).

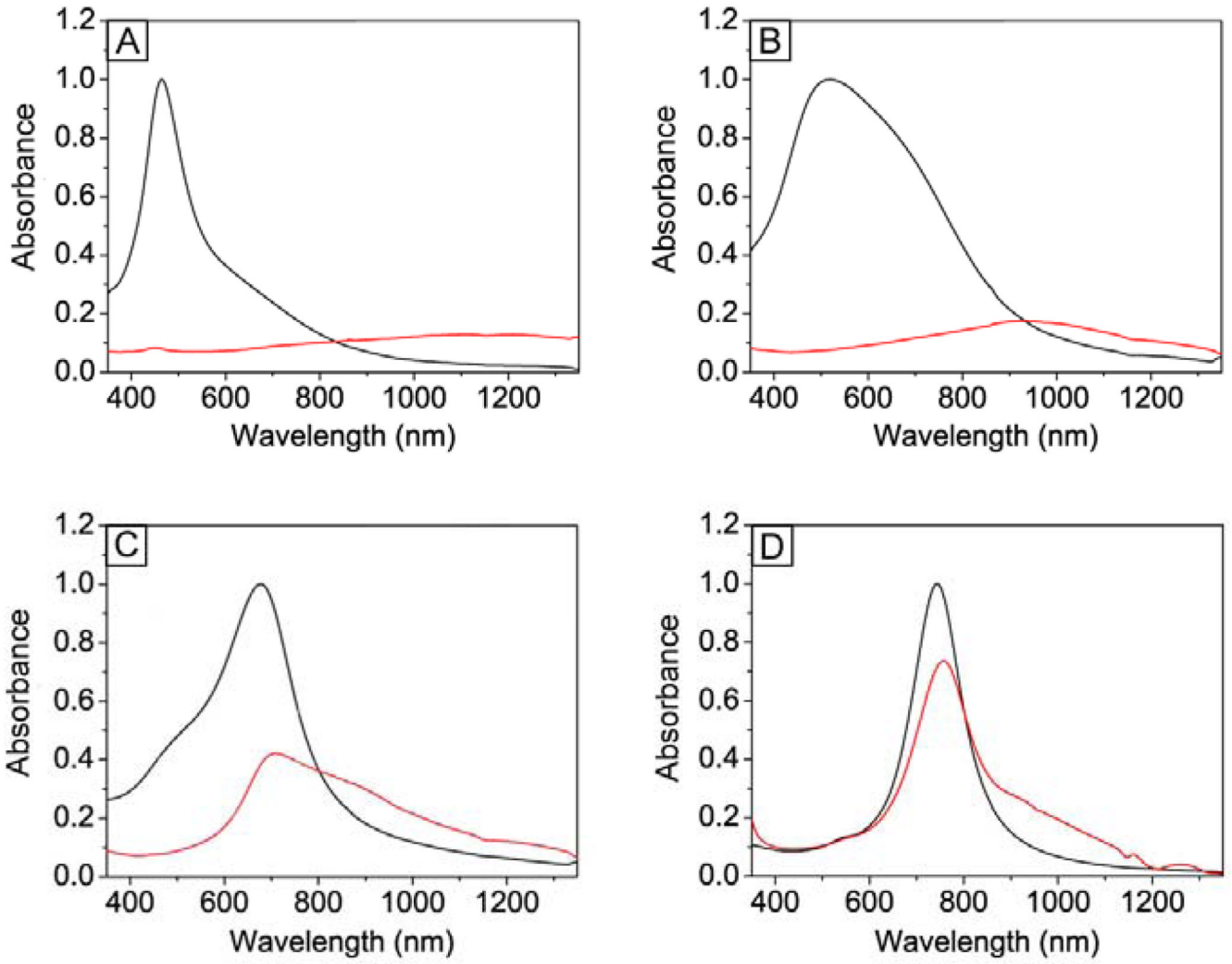

Figure 3.

UV-vis-NIR spectra of the samples that correspond to the Au-Ag alloy nanoboxes and nanocages shown in Figure 1. The spectra in black are for the starting Au-Ag nanoboxes and the spectra in red are for the resulting Au-based nanocages after a reaction with an excess amount of H_2O_2. For the nanoboxes, the LSPR peaks were at (A) 460, (B) 520, (C) 675, and (D) 745 nm. The spectra were normalized to unity. For the nanocages, the LSPR peak was red-shifted to the near-infrared region for the first two samples of nanocages due to their extremely thin walls. The spectra were normalized by dividing the same factor to the corresponding spectra of the nanobox.

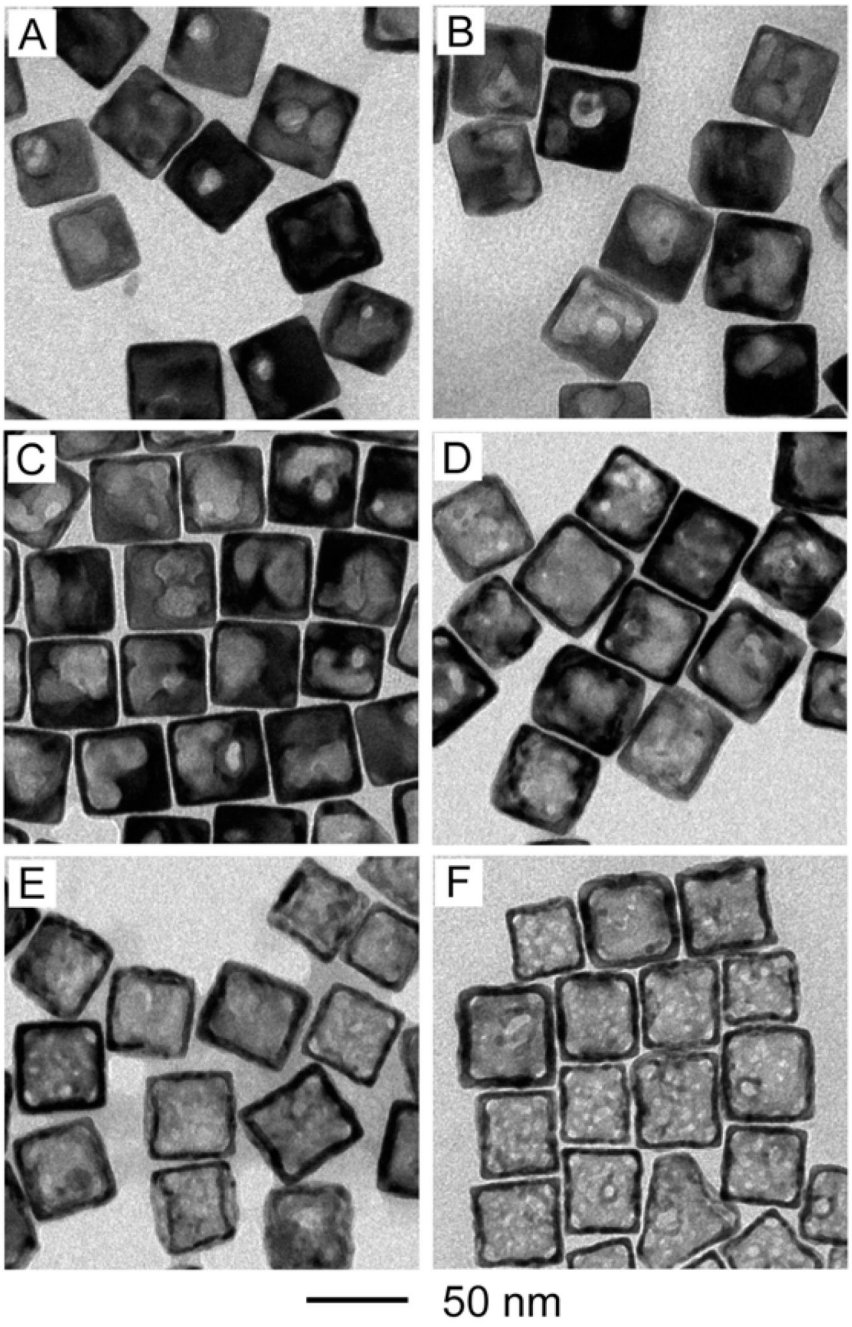

Figure 4.
TEM images of Au-based nanocages after a suspension of Au-Ag alloy nanoboxes (with an LSPR peak at 520 nm) had been titrated with different volumes of 10 mM H_2O_2: (A) 0, (B) 10, (C) 20, (D) 30, (E) 40, and (F) 50 μL.

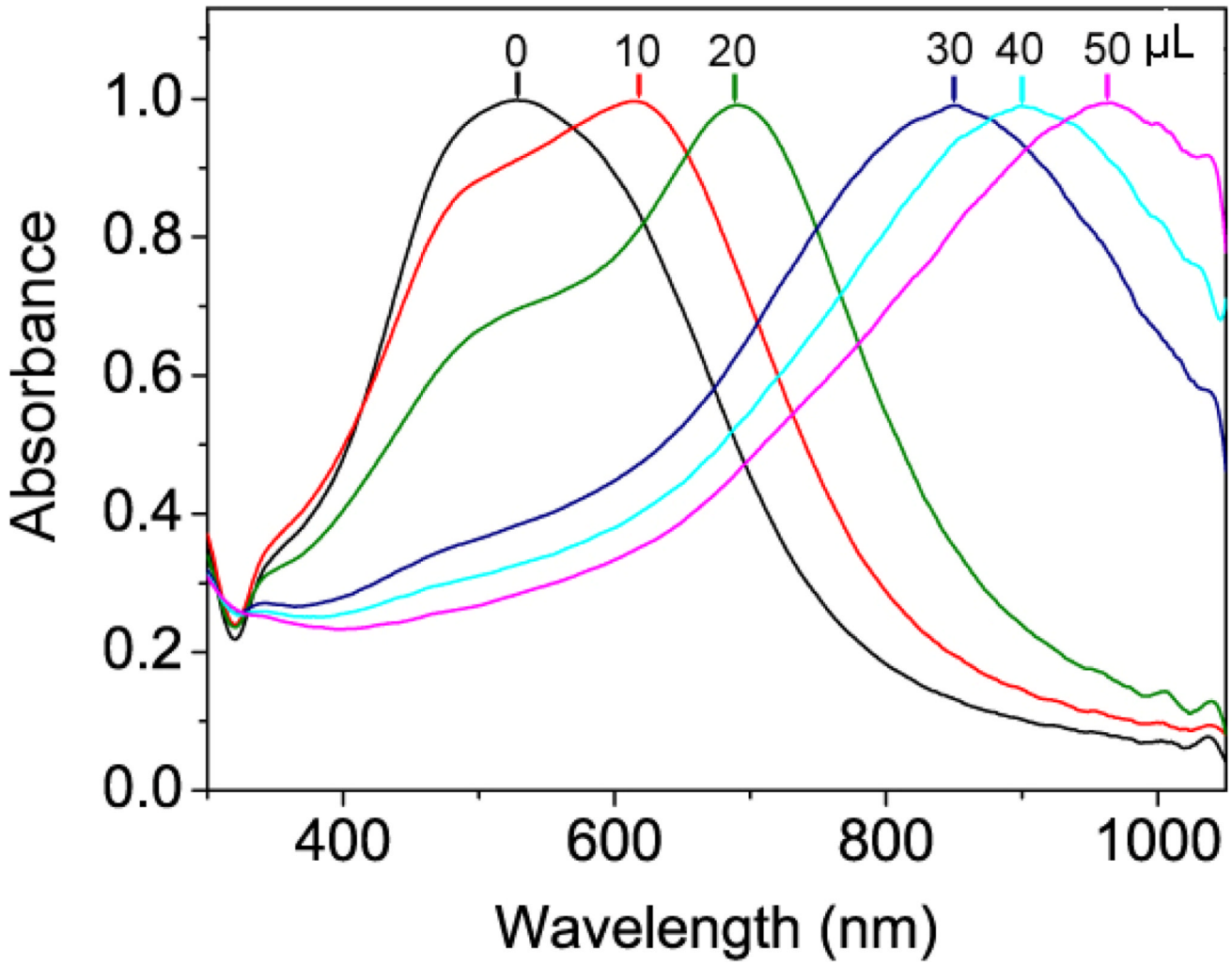

Figure 5.
UV-vis spectra that correspond to different stages of the titration process shown in Figure 4. The spectra were normalized to unity.

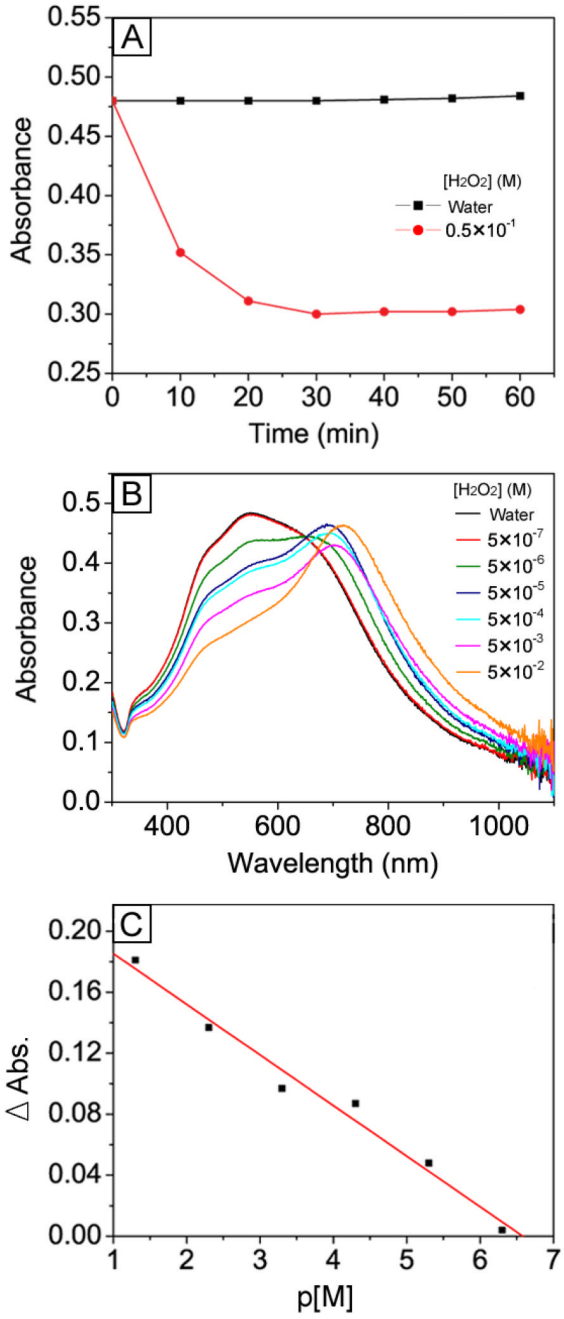

Figure 6.

H_2O_2 detection based on changes to the optical properties of Au-Ag nanoboxes. (A) Plots of intensity of absorbance at 545 nm as a function of incubation time. (B) UV-vis-NIR spectra of the Au-Ag nanoboxes (with an LSPR at 545 nm) after incubation with H_2O_2 at different concentrations for 30 min. (C) A plot of intensity change (ΔAbs) of extinction at 545 nm as a function of concentration (−log [M] or p[M]), ΔAbs = 0.28 − 0.03 × p[M], R^2 = 0.99).